Ultra-broadband plasmonic perfect absorber based on titanium-aluminum oxide strip multilayer structure

F. CHEN*, Y. XU
School of Physics and Optoelectronic Engineering, Yangtze University, Jingzhou, 434023, China

In this paper, an ultra-broadband perfect absorption has been demonstrated by using titanium-aluminum oxide ($Ti-Al_2O_3$) strip grating metamaterial structure in the visible and near-infrared region. Numerical simulations of the finite-difference time-domain (FDTD) method indicate that perfect absorption with an average absorbance of 96.8 % can be achieved from 471 nm to 2278 nm, with 90 % absorption bandwidth over 1807 nm and the peak absorption is up to 99.6 %. Ultra-broadband perfect absorption is achieved due to the excitation of localized surface plasmon resonance and propagating surface plasmon resonance. Angle independent up to 20^o of the proposed absorber is also investigated. Moreover, the effects of geometrical sizes and metal material on absorption performance are studied in details. The proposed absorber possess the advantages such as, ultra-broadband, high average absorption, easy fabricate and simple structure. The proposed ultra-broadband perfect absorber may find potential application in solar cell, plasmonic detection in infrared range.

(Received August 29, 2020; accepted February 10, 2022)

Keywords: Plasmonic resonance, Metamaterial, Ultra-broadband perfect absorption, Solar cell

1. Introduction

Metamaterial, a kind of man-made material with special properties, has attracted numerous research attention in recent years due to its unique physical properties [1-5]. With this motivation, a lot of plasmonic metamaterial nanodevices have been proposed and investigated, such as plasmonic tunable absorbers [6-7], plasmonic filters [8], plasmonic sensors [9], cloaking[10]. Plasmonic perfect absorber (PPA) has been attracted lots of attention since its wide application in plasmonic sensing, solar energy, optical imaging and detection [9,11-13]. There are numerous ways to enhance the absorption of incident light, such as surface plasmon polaritons and magnetic dipolar resonance, localized surface plasmon and FP cavity mode resonance [14-15].

Since the first PPA was proposed by Landy et al. in 2008 [16], many metallic nanostructures with either polarization-insensitive or polarization-sensitive absorption have been investigated theoretically and demonstrated experimentally. For example, in 2011, K. Aydin et al. investigated an absorber consisting of a metal-insulator-metal stack and crossed trapezoidal arrays, the absorber can improve the efficiency of solar cells in the visible range [17]. In 2018, Wang et al. numerically studied multispectral metamaterial absorbers based on a periodic sub wavelength array of nanogrooves side-coupled to nanorings [18]. Very recently, our group reported a tunable plasmonic perfect absorber based on multilayer graphene strip grating structure [19]. Further we also reported a double-band PPA based on dielectric grating and Fabry-Perot cavity [20]. Huang et al. proposed and studied ultra-broadband perfect absorbers based on dielectric semiconductor-metal trilayers structure in near-infrared range [21]. Compared to narrow band PPA, broadband PPA is more valuable in application such as photodetectors, thermal emitters and photovolatics [22-23]. In order to produce broadband PPA, Ti and Al are often used, since its price is much lower than Au and Ag, and the large imaginary part of dielectric function of Ti make it possess high loss, which is benefit to broadband PPA. For broadband PPA, Chen et al. proposed a highly efficient ultra-broadband perfect absorber with a *Al-SiO_2-Si-Ti* four-layer structure. Xu et al. proposed an ultra-broadband absorber based on a thin metamaterial nanostructure composed of a periodic array of *Ti-SiO_2* cubes, which show perfect absorption with average absorbance of 97% from visible to near-infrared.

In this paper, combined the *Ti-Al_2O_3* strip grating with uniform *Ti-Al_2O_3* layer and substrate, an ulta-broadband perfect absorber spanning a broad range from 471 to 2278 *nm* is achieved. The position of absorption bandwidth can be tuned by changing geometrical sizes such as the grating width, period and height. The designed ulta-broadband perfect absorber has excellent absorption stability over a wide angle range of incidence around $\pm 20^0$. The proposed metamaterial structure not only has a simple structure, low cost, ultra-broad bandwidth, but also can be fabricated with lithography and deposition methods. The results of this paper can find potential application in solar energy, thermal emitters and detection in the infrared range [24-27].

2. Model and theory

The proposed ultra-broadband perfect absorber is schematically illustrated in Fig. 1 (a), $Ti-Al_2O_3$ strip grating is placed on the surface of a uniform $Ti-Al_2O_3$ layer and coated with a Ti substrate. Fig. 1 (b) is the side view of unit cell of the proposed plasmonic absorber.

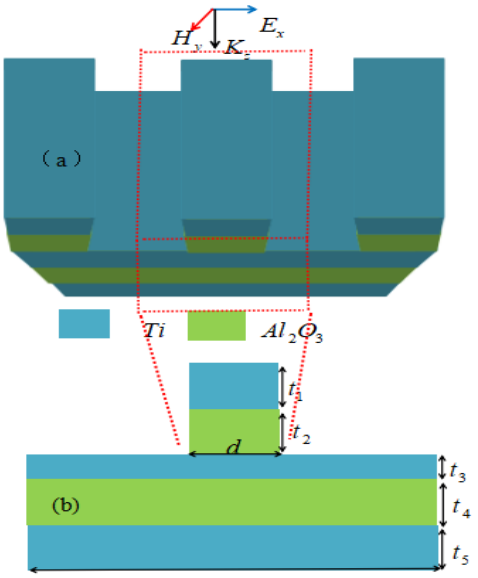

Fig. 1. (a) Schematic diagram of the proposed broadband plasmonic absorber, a periodic titanium-aluminum oxide strip is placed on the surface of a uniform MDM structure. (b) Unit cell of the side view of the proposed plasmonic absorber, p. d stand for the period, width of Ti-Al_2O_3 strip, t_1, t_2, t_3, t_4, and t_5 represent for the thickness of the Ti - Al_2O_3 strip, Ti layer, Al_2O_3 layer and Ti substrate (color online)

The geometrical parameters are as follows: The thickness of *Ti* strip, Al_2O_3 strip, *Ti* layer, Al_2O_3 layer and *Ti* substrate are t_1, t_2, t_3, t_4 and t_5. The period and width of *Ti*-Al_2O_3 strip are p and d. Due to the periodicity of the proposed structure, the simulation domain is made up of a single unit of the structure with periodic boundary conditions are imposed in the x and y direction, while in the Z direction, a perfectly matched absorption boundary condition is used. A plane wave source with polarization along x direction is normally incident from Z direction. With the transmittance ($T(\lambda)$) and reflectance ($R(\lambda)$) obtained from two 2D frequency-domain power monitors, the absorption ($A(\lambda)$) of the plasmonic absorber can be calculated by the relationship: $A(\lambda)=1-T(\lambda)-R(\lambda)$. In the proposed structure, as the 270 *nm* thick *Ti* substrate, the transmittance is almost zero, therefore the absorption $A(\lambda)$ can be represented by $A(\lambda)=1-R(\lambda)$. In the following FDTD simulations, the permittivity of the Al_2O_3 layer is set to 1.76. The frequency-dependent complex permittivity of *Ti* is from Palik [28].

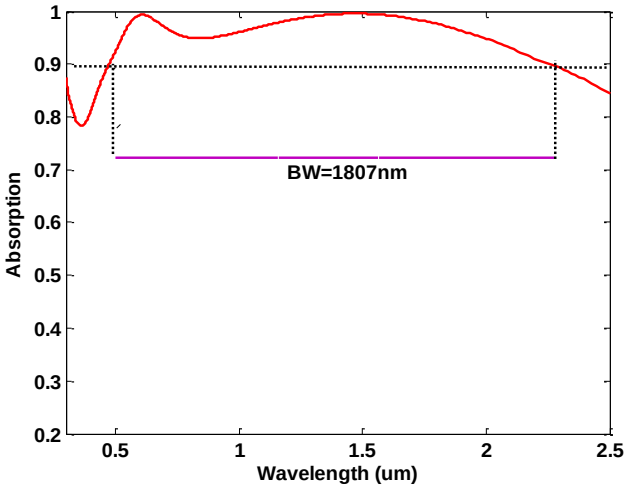

Fig. 2. FDTD calculated absorption spectra of the proposed structure with TE polarization. The geometrical parameters are: $t_1=117\,nm$, $t_2=23\,nm$, $t_3=10\,nm$, $t_4=120\,nm$, $t_5=270\,nm$, $p=300\,nm$, $d=120\,nm$

Fig. 2 shows the numerically calculated absorption spectra with $t_1=117\,nm$, $t_2=23\,nm$, $t_3=10\,nm$, $t_4=120\,nm$, $t_5=270\,nm$, $p=300\,nm$, $d=120\,nm$. It can be noticed that the proposed absorber exhibits a high absorption over 90% in a wide wavelength range from 471 *nm* to 2278 *nm*. The 90% bandwidth is about 1807 *nm*, the average absorption is calculated by $A=\int_{\lambda_2}^{\lambda_1}A(\lambda)d\lambda/(\lambda_1-\lambda_2)$, where λ_1 and λ_2 are 2278 nm and 471 *nm*, respectively. The average absorbance over this band is about 96.5%. And two absorption peaks at 609 *nm* and 1479 *nm*, with corresponding absorptance about 99.4% and 99.6%, respectively. The bandwidths and absorption efficiency are better than other related plasmonic absorbers structures [29-30]. To investigate the physical mechanism of the ultra-broadband perfect absorption effect, we examined the steady-state electric field $|E|^2$ and magnetic field $|H|^2$ distributions of the unit cell. Fig 3 (a)-(d) shows the magnetic field $|H|^2$ distributions of the section $x-y$ plane for four wavelengths $\lambda=1.19\,\mu m, 1.39\,\mu m, 1.7\,\mu m, 2.05\,\mu m$.

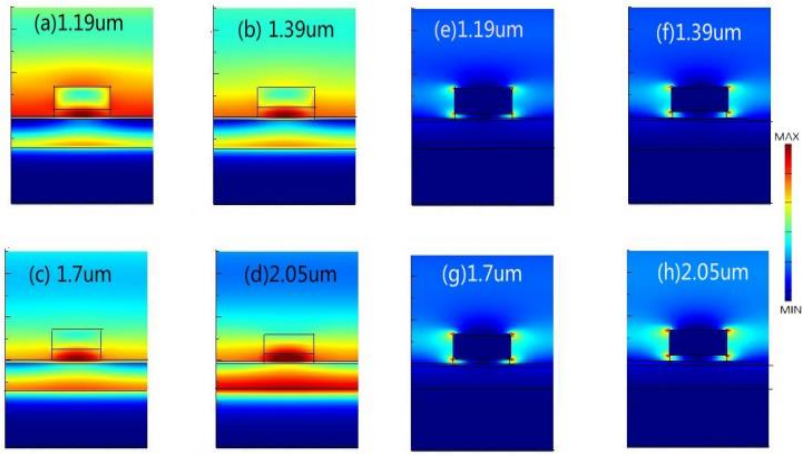

Fig. 3. Numerically simulated distribution of magnetic field ($|H|^2$) (a)-(d), electric field ($|E|^2$) (e)-(h) of the section $x-z$ plane at $y=0$ for four wavelengths $\lambda = 1.19\,\mu m, 1.39\,\mu m, 1.7\,\mu m, 2.05\,\mu m$ (color online)

In Fig. 3 (a), at short wavelength of 1.19 μm, one part of magnetic field is strongly confined in the Al_2O_3 strip under the Ti strip, another part of magnetic field is strongly confined in the air gap between neighbouring cells, which implying that the perfect absorption at short wavelength is originated from the excitation of propagating surface plasmon. At long wavelength 2.05 μm, from Fig. 3 (d) it can be noticed that the magnetic field is strongly confined in the Al_2O_3 strip and the lower Al_2O_3 layer. Localized surface plasmon leads to the perfect absorption. From Fig. 3 (b) and (c), the absorption is originated from the hybridization between localized surface plasmon and propagating surface plasmon. Fig. 3 (e)-(h) depict the steady state electric field $|E|^2$ of of the the section $x-y$ plane, it can be noticed that two dipoles resonance are occurred and electric field distributions confined at the edges of upper and lower surfaces of the Ti strip along X direction. Since the Ti layer is only 10 nm, the input electromagnetic wave bounces back between the top Ti strip and lower Ti substrate, just like a Fabry-Perot resonator with low quality factor (Ti is a highly lossy metal), the combination of FP resonance, localized surface plasmon and propagating surface plasmon make the absorption bandwidth broaden. For TM polarization, Figs. 4 and 5 show the numerically calculated absorption spectra and field distributions. It can be noticed that the proposed absorber exhibits a secondary absorption about 56% in the wavelength of interest. Since the proposed structure is infinite in y direction without centrosymmetry, therefore the proposed absorber is polarization dependence.

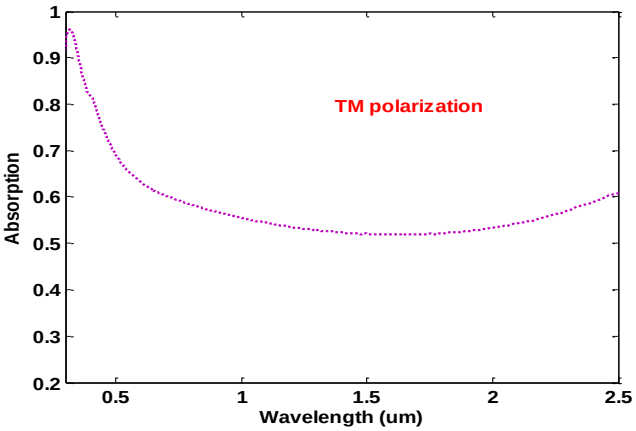

Fig. 4. FDTD calculated absorption spectra of the proposed structure with TM polarization, the other geometrical parameters are the same with Fig. 2

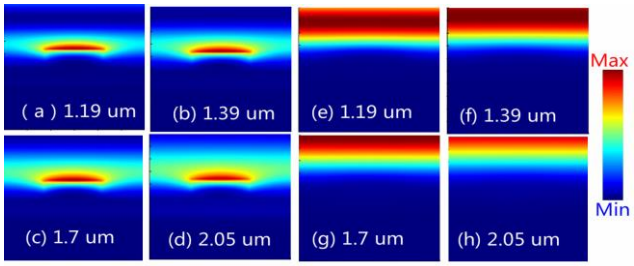

Fig. 5. Numerically simulated distribution of magnetic field ($|H|^2$) (a)-(d), electric field ($|E|^2$) (e)-(h) with TM polarization (color online)

To investigate the influence of geometrical sizes on the absorption performance of the proposed structure. Fig. 6(a) shows the evolution of the absorption with the

parameter *d*. It can be observed that when the width of the *Ti*-Al_2O_3 strip increases from *d* = 100 *nm* to 140 *nm* with fixed *p* = 300 *nm*, the corresponding two absorption peaks are red shifted and the absorption peak at the long wavelength redshift more obvious, therefore, the bandwidth are broaden with increasing the width d. And the absorptance between the two absorption peaks decreased with the increase of *d*. Fig. 6 (b) shows the absorption spectra of the proposed structure with various *p*, when the period decreases from *p* = 300 *nm* to 220 *nm*, the bandwidth increases and the absorptance between the two absorption peaks decreased. This characteristic indicates that the absorption performance of the proposed absorber can be tuned by changing the width and the period.

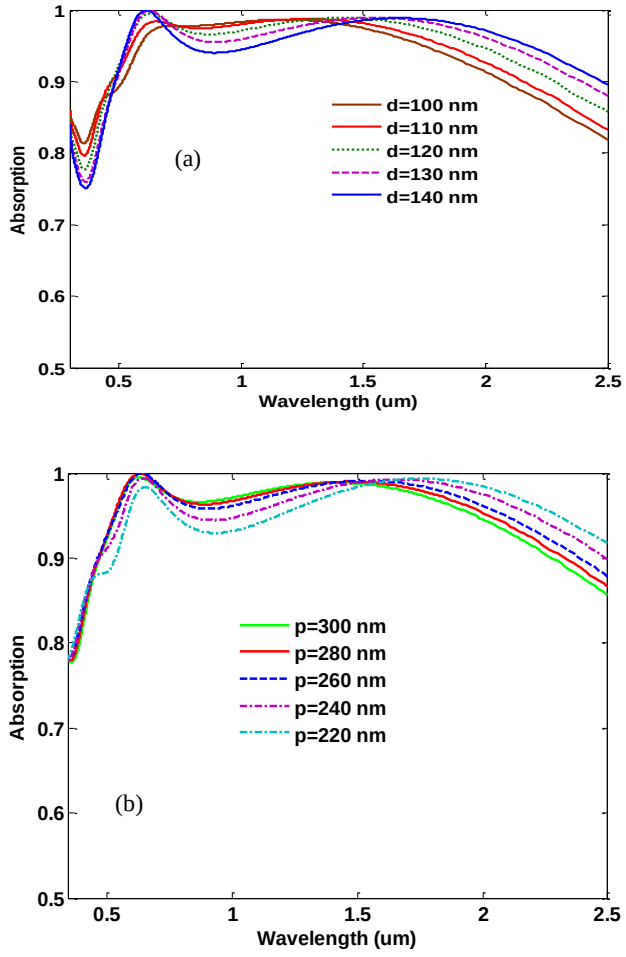

Fig. 6. Numerical calculated absorption spectra of the proposed structure with various geometrical sizes (a) the width of Ti-Al_2O_3 strip d from 100 nm to 140 nm (b) the period p from 300 nm to 220 nm (color online)

The absorption spectra with different *Ti* strip heights t_1 are showed in Fig. 7(a), it can be seen that when the height of the *Ti* strip increases from $t_1 = 97\ nm$ to 137 *nm*, the corresponding absorptance increases but the bandwidth decrease as well, this is because *Ti* is a highly lossy metal material, a thinner *Ti* strip means a lower lossy and a stronger coupling. With increasing $t_1 = 97\ nm$ to 137 *nm*, the average absorption increases from 95.8% to 96.3%, 96.8%, 97.4% and 97.8%. Therefore, the height of *Ti* strip in the proposed absorber was selected 117 *nm*. The absorption spectra with different Al_2O_3 layer heights t_4 are showed in Fig. 7(b), it can be seen that when the height of the Al_2O_3 layer increases from $t_4 = 120\ nm$ to 160 *nm*, the corresponding absorption band red shifts. This is because the effective resonance wavelength of FP cavity increases as t_4 increases. With increasing $t_4 = 120\ nm$ to 160 *nm*, the average absorption decreases from 96.8% to 96.3%, 95.9%, 95.4% and 95.1%. Therefore, the absorption peaks can be tuned by changing the heights of the *Ti* strip and Al_2O_3 layer.

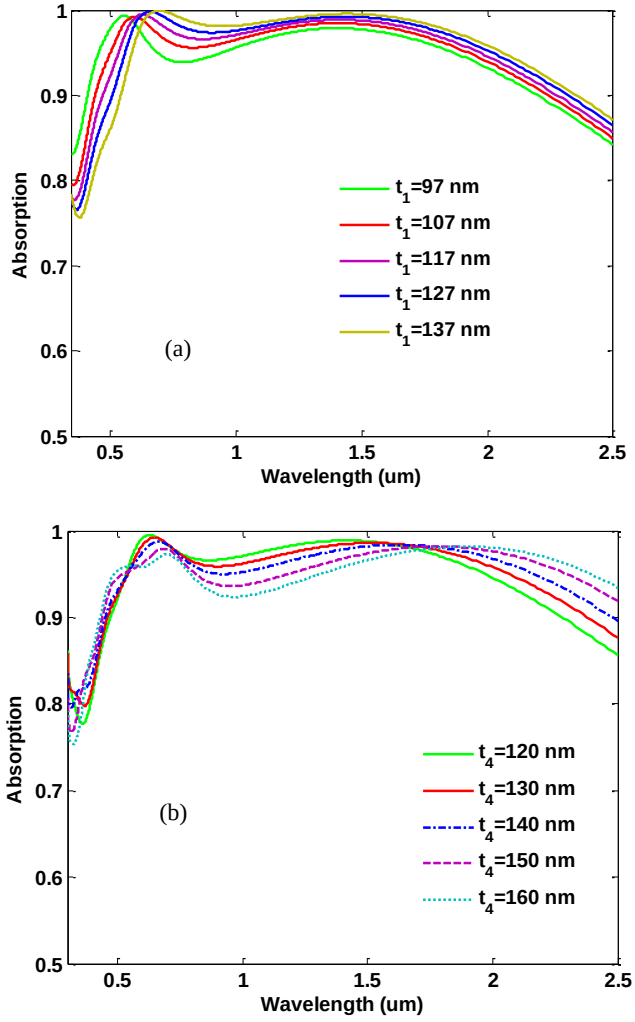

Fig. 7. Numerical calculated absorption spectra of the proposed structure with various heights of the Ti strip t_1 and Al_2O_3 layer t_4 (color online)

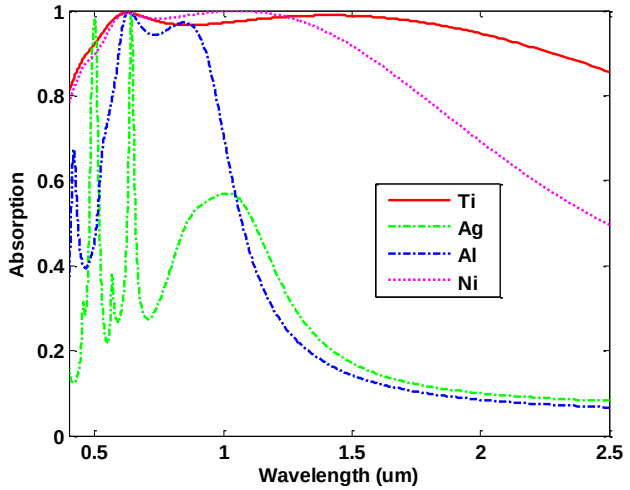

Fig. 8. Absorption spectra with different metals, the Ti is replaced by silver (Ag), aluminum (Al), nickel (Ni) (color online)

For a thorough study, we investigate the impact of metal material by replacing the Ti with several commonly used metals while keeping the geometry parameters constant. It can be noticed that the metal largely affects the performance of the proposed absorber. When using aluminum and silver, the absorption spectra exhibit narrow resonances around 635 *nm*/853 *nm* or 501 *nm*/644 *nm*, corresponding to the FP and SPP resonances. When using nickel, the absorption spectra exhibit even higher but the absorption band is up to 1251 *nm*. Since the top metal layer is not only related to the Q factor of the FP resonance cavity, but also the coupling strength of the cavity mode, the intrinsic dispersion property and highly lossy of Ti lead to a high absorption over 90% in a wide wavelength range from 471 *nm* to 2278 *nm*.

To investigate the incident angle on the absorptance of the proposed structure. As shown in Fig. 9, incident angle is increased from 0^0 to 40^0, the spectral absorption are almost no change under 20^0, but the bandwidth decreases as the incident angle increases to 30^0 and 40^0. Since the proposed structure is highly symmetrical in x direction, the proposed plasmonic absorption response is retained well in a wide angle range ± 20^0. Fig. 9 (b) shows the average absorption as a function of the incident angle. With increasing the incident angle from 0^0 to 60^0, the average absorption decreases from 96.8% to 96.7%, 96.3%, 95.9%, 95.3%, 95.1% and 94.8%, the results indicate that the proposed plasmonic absorption is independent in a wide incident angle. These characteristics are valuable for applications in the solar cell, since in real system, the incident angle of solar light is unequal.

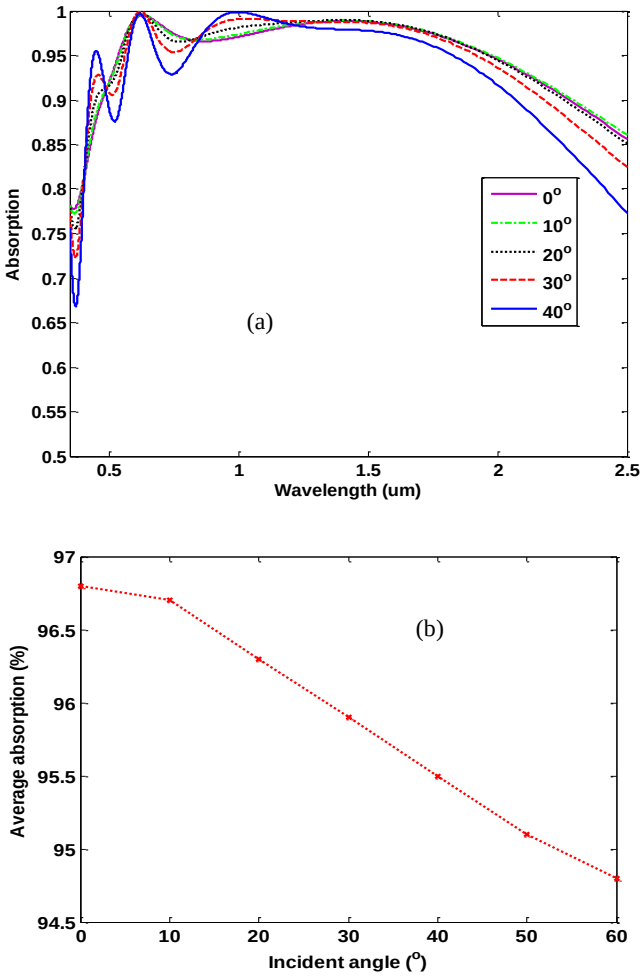

Fig. 9. (a) Absorption spectra with different incident angles from 0^0 to 40^0. (b) Average absorption as a function of the incident angle (color online)

3. Conclusion

In conclusion, an ultra-broadband plasmonic absorber based on *Ti - Al_2O_3 – Ti - Al_2O_3 - Ti* five-layer structure has been studied numerically. Results show that bandwidth of absorption over 90% can reach 1.8 μm. The combination of FP resonance, localized surface plasmon and propagating surface plasmon in the two MIM absorbers leads to the ultra-broadband absorption. The absorption average remains higher than 94.8% with an incident angle up to 60^0. Effect of geometrical sizes, such as the strip width, period and height on the absorption performance is studied in detail. Effects of different metal materials on the absorption performance are compared to investigate the characteristics of the proposed absorbers. The proposed absorber possess advantages such as, ultra-broadband, high average absorption, easy fabricate and simple configuration. Without using noble metal resulting in low manufacturing process cost. It is believed that the proposed absorber has potential application solar energy, thermal emitters and detection in the infrared range.

Acknowledgements

Supported by The Yangtze Youth Fund (Grant No. 2016cqn55), Yangtze Fund for Youth Teams of Science and Technology Innovation (Grant No. 2015cqt03). National Natural Science Foundation of China (Grant No. 11747091). Supported by the talent and high level thesis cultivation program of School of physics and Optoelectronics Engineering, Yangtzeu University.

References

[1] K. F. MacDonald, Z. L. Samson, M. I. Stockman, N. I. Zheludev, Nat. Photonics **3**, 55 (2009).
[2] G. X. Wang, H. Lu, X. M. Liu, D. Mao, L. N. Duan, Opt. Express **19**, 3513-18 (2011).
[3] F. Chen, H. F. Zhang, L. H. Sun, J. J. Li, C. C. Yu, Opt. Laser. Technol. **116**, 293 (2019).
[4] J. Zhou, L. Jin, E. Y. B. Pun, Optics Letters **37**, 2613 (2012).
[5] A. J. Abdul, W. Bernd, Plasmonic **9**, 1265 (2014).
[6] Y. Bai, L. Zhao, D. Q. Ju, Y. Y. Jiang, L. H. Liu, Opt. Express **23**(5), 8670 (2015).
[7] H. Tao, C. M. Bingham, A. C. Strikwerda, D. Pilon, D. Shrekenhamer, N. I. Landy, K. Fan, X. Zhang, W. J. Padilla, R. D. Averitt, Phys. Rev. B **78**, 241103 (2008).
[8] F. Chen, D. Z. Yao, J. Mod. Opt. **61**, 1486 (2014).
[9] N. Liu, M. Mesch, T. Weiss, M. Hentschel, H. Giessen, Nano Lett. **10**, 2342 (2010).
[10] X. Ni, Z. J. Wong, M. Mrejen, Y. Wang, X. Zhang, Science **349**, 1310 (2015).
[11] H. X. Zeng, Z. G. Li, L. Stan, D. Rosenmann, D. Czaplewski, J. Gao, X. D. Yang, Opt. Lett. **40**, 2592 (2015).
[12] X. L. Liu, T. Talmage, S. Tatiana, F. S. Anthony, M. J. Nan, J. P. Willie, Phys. Rev. Lett. **107**, 045901 (2011).
[13] Z. Jun, Q. Liuli, S. Shuxiang, Z. Junwen, L. Siyuan, Photonic Sensors **5**, 159 (2015).
[14] B. Zhang, Y. Zhao, Q. Hao, B. I. C. Kiraly Khoo, S. Chen, T. J. Huang, Opt. Express **19**, 15211 (2011).
[15] M. Y. Huang Cheng, Z. Cheng, X. Mao, R. Gong, Opt. Commun. **415**, 194 (2018).
[16] N. I. Landy, S. Sajuyigbe, J. J. Mock, D. R. Smith, W. J. Padilla, Phys. Rev. Lett. **100**, 207402 (2008).
[17] K. Aydin, V. E. Ferry, R. M. Briggs, H. A. Atwater, Nat. Commun. **2**, 517 (2011).
[18] H. J. Li, Z. R. Ren, P. Meng, L. L. Wang, J. Appl. Phys. **123**, 20312 (2018).
[19] F. Chen, D. Z. Yao, H. F. Zhang, L. H. Sun, C. C. Yu, Journal of Electronic Materials **48**, 5603 (2019).
[20] F. Chen, H. F. Zhang, L. H. Sun, J. J. Li, C. C. Yu, Appl. Phys. A **125**, 792 (2019).
[21] Y. J. Huang, L. Liu, M. B. Pu, X. Li, X. L. Ma, X. G. Luo, Nanoscale **10**, 8298 (2018).
[22] Y. Gong, Z. Wang, K. Li, L. Uggalla, J. Huang, N. Copner, Y. Zhou, D. Qiao, J. Zhu, Opt. Lett. **42**, 4537 (2017).
[23] A. Vora, J. Gwamuri, N. Pala, A. Kulkarni, J. M. Pearce, D. O. Guney, Sci. Rep. **4**, 4901 (2015).
[24] Y. S. Zhu, H. X. Xu, P. Yu, Z. M. Wang, Applied Physics Reviews **8**(2), 021305 (2021).
[25] Y. S. Zhu, P. Yu, T. J. Liu, H. X. Xu, A. O. Govorov, Z. M. Wang, ACS Applied Electronic Materials **3**(2), 639 (2021).
[26] Y. S. Zhu, P. Yu, E. Ashalley, T. J. Liu, F. Lin, H. N. Ji, J. C. Takahara, A. Govorov, Z. M. Wang, Nanotechnology **31**(27), 274001 (2020)
[27] P. Yu, L. V. Besteiro, Y. J. Huang, J. Wu, L. Fu, H. H. Tan, C. Jagadish, A. Wiederrecht, A. O. Govorov, Z. M. Wang, Advanced Optical Materials **7**(3), 1800995 (2019).
[28] E. D. Palik, Handbook of Optical Constants of Solids, Academic Press, Orlando, Florida 1985.
[29] J. W. Cong, Z. Q. Zhou, B. F. Yun, L. Lv, H. B. Yao, Y. H. Fu, N. F. Ren, Opt. Lett. **41**, 1965 (2016).
[30] Z. Y. Li, P. Edgar, B. Serkan, K. Hasan, A. Koray, Nano Lett. **5**, 15137 (2015).

*Corresponding author: 501110@yangtzeu.edu.cn